
SHIELD TUNNELLING 3D NUMERICAL SIMULATION ON THREE CASE STUDIES

Rafik Demagh^{1*}, Fabrice Emeriault² & Farid Hammoud¹

¹University of Batna, Civil Engineering Department, Algeria

²Grenoble-INP, UJF-Grenoble 1, CNRS UMR 5521, 3SR, Grenoble F-38041, France

*Corresponding Author: rafik.demagh@univ-batna.dz

Abstract: In congested urban areas, shallow tunnel constructions are sometimes necessary due to lack of space. Therefore, a careful assessment of their effects on existing constructions is vitally required. In the application of shield tunnel boring machines (TBM), different operations conducted may induce a three-dimensional problem of soil/structure interaction. They are complicated to be represented in a complete numerical simulation that allows evaluation of induced ground movements, in particular surface settlement assessment. A three-dimensional simulation procedure, using finite differences code Flac-3D, taking into account an explicit manner of the main origins of movements in soil mass, is hereby presented in this paper. It is applied to three different tunnel construction sites, with different types of face support and soils (i.e. nature and mechanical characteristics). Results have been compared to those obtained from in-situ measurements during construction. It shows that the proposed 3D simulation procedure is highly relevant, particularly in the adopted representation for different operations performed by tunnel boring machine (excavation, confining pressure, advancement, installation of lining, grouting of annular void, etc.).

Keywords: Tunnel boring machine (TBM), 3D numerical simulation, confining pressure, grouting, in-situ monitoring.

1.0 Introduction

The ground movements induced by shield TBM tunnelling (i.e. deformations of surrounding tunnel ground and surface settlement) are due to a complex sequence of operations: excavation, front support, shield advancement, grouting of annular void, grout percolation along the shield and grout consolidation. As a result, explicit numerical simulation of tunnelling processes is quite difficult. During the last decade, several 3D phased simulation of tunnel boring process, generally for soft and saturated soils, have been proposed by various authors (Broere and Brinkgreve, 2002; Dias *et al.*, 2000; Kasper and Meschke 2004 & 2006; and, Mroueh and Shahrouh, 1999 & 2008). The comparison with observations results performed on tunnel construction sites shows

that, in spite of progress in terms of means and computing time, tunnelling-induced phenomena are still not well known.

This article proposes an explicit 3D simulation procedure to analyse processes that occur around a TBM during tunnelling. The latter is applied to three construction sites with different tunnels related parameters regarding shields size, face support type (slurry shield or earth pressure balance), crossed soils nature and mechanical characteristics. The comparison with results obtained from observations made on these construction sites shows that the proposed versatile numerical procedure is able to consider all the complexities of the tunnelling induced movements.

2.0 Construction Sites Description

Three construction sites, namely, Line D of Lyon's subway (Benmebarek and Kastner, 2000), Line B of Toulouse's subway (Vanoudheusden, 2006) and Shanghai Yangtze River Tunnel (Yan *et al.*, 2008), for which reliable in-situ measurements results are available, have been selected for comparison and qualification. Figure 1 and Table 1 summarize respectively the main geometrical notations and parameters values of tunnels, shields and liners used in this study.

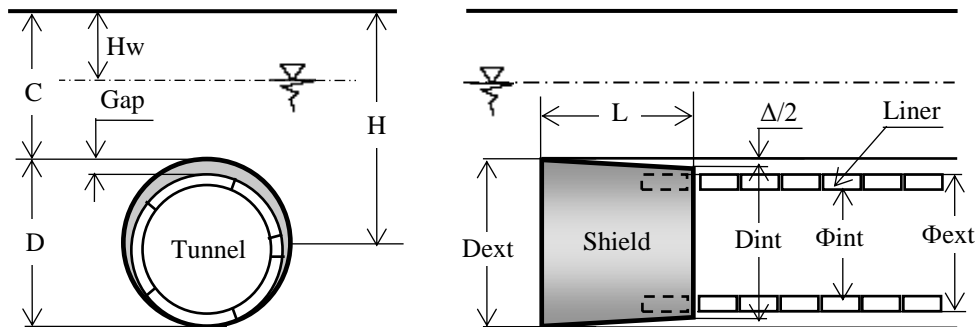


Figure 1: Tunnel, shield and liner geometrical notation

Table 1: Tunnel, shield and liner parameters

Case	Tunnel			Shield						Liner			
	H m	D m	C/D	H _w m	Gap cm	Dext m	Dint m	L m	Δ/2 mm	Φext m	Φint m	Width cm	Thickness cm
Lyon	13.6	6.3	1.66	3	27	6.27	6.24	6.0	15	6.0	5.3	100	35
Toulouse	16.5	7.7	1.64	4	20	7.7	7.65	8.4	25	7.5	6.8	140	35
Shanghai	17.5	15.43	0.64	5.5	23	15.43	15.26	14	85	15.2	15.07	200	65

2.1 Case of Line D of Lyon's subway

The slurry shield TBM with a diameter of 6.3 m, crosses heterogeneous alluvial soils, constituted of normally consolidated and fairly permeable silts. Table 2 summarizes geotechnical parameters of crossed materials. The P2-S section is chosen for a comparison with measurements made.

Table 2: Soil geotechnical parameters for Lyon case

Layer	Depth m	γ kNm ⁻³	K_0	c' kPa	ϕ' degrees	ψ' degrees	E MPa
Fill	0-3	19	0.5	30	30	17	7.8
Brown Silt	3-5	21	0.5	10	25	15	7.3
Beige silt	5-8	21	0.5	15	32	20	7.3
Ocher silt	8-12	21	0.5	15	25	14	7.3
Grey silt	12-15	21	0.5	5	30	14	4.2
Sands	15-18.5	21	0.5	0	34	20	28
Gneiss	18.5-20	21	0.5	150	45	30	140

(Source: Benmebarek and Kastner, 2000)

2.2 Case of Line B of Toulouse 's subway

The EPB's TBM (earth pressure balanced shield) with a diameter of 7.7m, crosses essentially highly over consolidated argillaceous soils, with a very low permeability (10^{-8} to 10^{-9} m/s). The "Toulouse's molasse" is characterized by a strong undrained shear strength c_u equal to 300 kPa. In particular, Young modulus is constant in the first 10 m and is equal to 165 MPa, and then increases with depth according to linear relationship $E(z) = E_0 + z.\Delta E$ with $E_0 = 66.1$ MPa and $\Delta E = 9.9$ MN/m³ (Table 3). Based on triaxial test results, this profile has been validated by numerical back-analysis on another monitoring section with similar geological context but excavated using conventional method. The "Castéra" section is considered for a comparison with measurements made.

Table 3: Soil geotechnical parameters for Toulouse case

Layer	Depth m	γ kNm ⁻³	K_0	c_u kPa	ϕ_u degrees	E MPa	ν
Fill	0-4	20	0.5	0	25	25	0.30
Molasse	4-10 >10	22	1.7	300	0	165 E(z)	0.45

(Source: Vanoudheusden *et al.*, 2006).

2.3 Case of Shanghai Yangtze River Tunnel

The slurry shield TBM with a diameter of 15.4 m is currently the largest one in the world. It crosses normally consolidated soft clays. Table 4 summarizes geotechnical parameters of crossed soils.

Table 4: Soil geotechnical parameters for Shanghai case

Layer	Depth m	γ kNm ⁻³	K_0	c' kPa	ϕ' degrees	c_u kPa	E MPa
Fill	0-7.5	17.5	0.5	13	18	0	2.84
Grey muddy silty clay	7.5-14	17.5	0.546	17	20	25	3.60
Grey muddy clay	14-27.5	17.5	0.546	14	18.1	23	2.21
Grey clay	27.5-32.5	18.5	0.546	22	21.1	41	4.24
Grey silty clay	32.5-47.5	18.5	0.546	12	25.9	42	6.18

(Source: Yan *et al.*, 2008).

3.0 Numerical Simulation Procedures

The 3D procedure proposed in Figure 2 for simulation of the phased excavation attempts to describe accurately all operations carried out by TBM and associated phenomena. It is implemented in commercial numerical code FLAC3D. Using TBM operation parameters recorded during the passage under monitoring sections, this procedure is repeated throughout shield progression until a stationary regime is reached (Demagh *et al.*, 2008). The simulations are carried out in drained conditions for Lyon case and in undrained conditions for Toulouse and Shanghai cases.

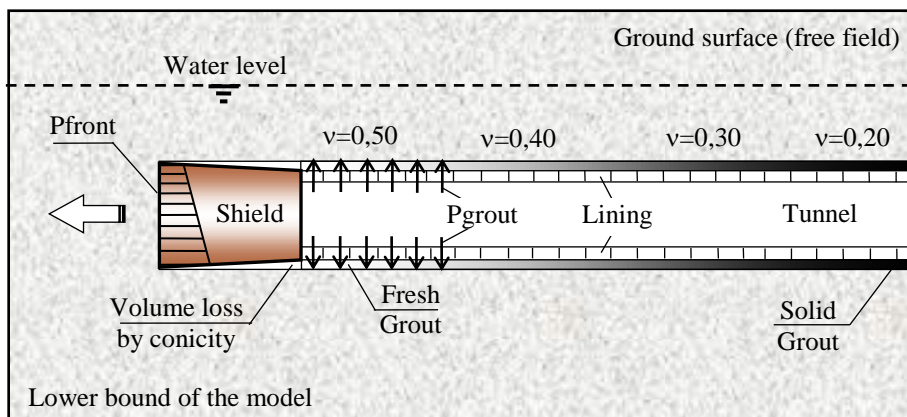


Figure 2: Complete phased simulation of TBM excavation process

The mesh shown in Figure 3 is composed of brick elements with eight nodes (75000 nodes at most for Toulouse case). The boundary conditions are imposed in terms of null displacements in perpendicular direction to the faces. The mesh extent, in longitudinal direction, is conditioned by the position of stationary section. The vertical symmetry allows limiting the model size. The soils are modelled in elastic plasticity with Mohr-Coulomb yield criterion and a non-associated flow rule requiring few parameters. A shield of conical shape, perfectly rigid (the nodes are fixed according to the method called fixed center (Benmebarek and Kastner, 2000), modelled with thin volumetric elements, is installed in a virgin ground solid mass for which an initial state of geostatic stresses is imposed with a coefficient of lateral earth pressure K_0 . When shield is completely installed, as illustrated in Figures 3, procedure of Figure 2 can be applied.

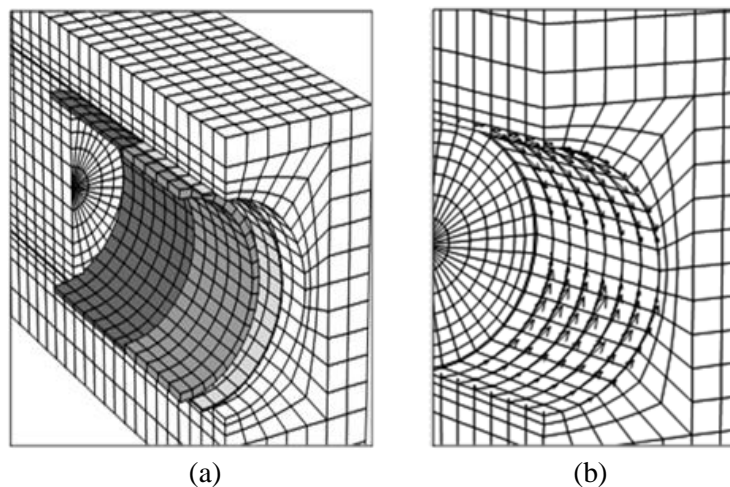


Figure 3: Meshing used in finite element modelling
 (a) View of different parts, (b) Arch effect of the displacements at the soil/shield interface

The assumption of a fixed centre seems to be verified in Figure 4: shield installation is characterized by the fact that, in the absence of injection, annular void is completely closed for considered cases, since the same displacements scales at the crown, springline and invert of the tunnel are obtained. However deformations do not evolve in the same way: excavation convergence is uniform in the case of Toulouse and Shanghai tunnels (homogeneous layer) and this is not the case in Lyon section (heterogeneous layers). As a result of poor quality of crossed grounds for Lyon and Shanghai cases a very weak damping of vertical displacements is noted. It is noticed that vertical settlements go up on the surface (Figures 4a and 4c), whereas in the case of Toulouse, these movements are confined in excavation vicinity (Figure 4b).

The excavation is simulated by deactivation of soil disk elements. The stability of front face is controlled by a normal pressure, noted P_{front} , presenting a gradient with depth,

interdependent of shield and progresses with the latter. This confining pressure profile, must respect instructions of pressure thresholds recorded on construction sites supports.

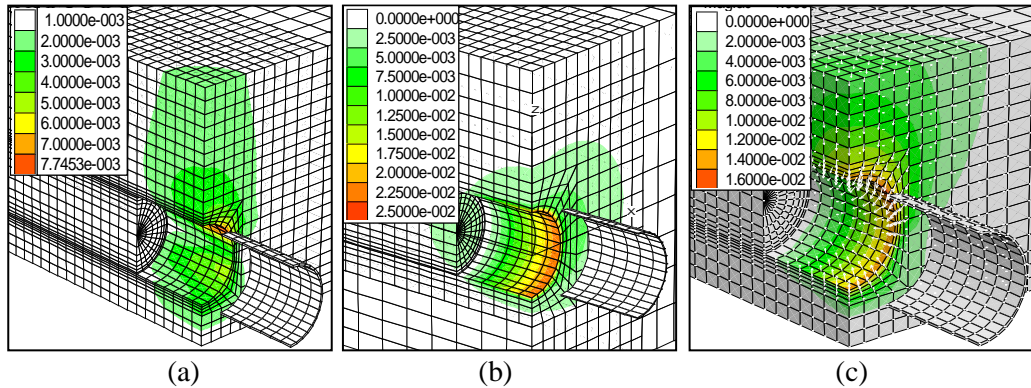


Figure 4: Contour of vertical displacement after complete installation of the shield
(a) Lyon case, (b) Toulouse case and (c) Shanghai case

The shield passage, simulated by annulment of local tangential stresses, clears a volume loss that is immediately filled by soil convergence (taking into account large displacements, Figures 3b and 4). The interface which is interdependent with shield is activated as soon as a contact is established with the surrounding ground; the role of this interface is to block radial convergence of ground and also to allow tangential convergence by transverse deformation arch effect (Figure 3b). The volume loss is partially compensated by possible migration of grout towards front of shield (there is a great uncertainty on post-closing shape of ground around shield). Two techniques are used to simulate this migration; either by a pressure applied over a certain length at the back of shield, or by a correction of the shield conicity, set so as to reproduce a vertical displacement recorded on construction site (back analysis on surface and/or tunnel crown vertical displacement). According to (Dias *et al.*, 2000), this second technique is more relevant.

The liner can be modelled either by shell or volumetric elements. It is characterized by a lower Young modulus value in order to take into account joints between the liner prefabricated rings. The injection of grout in annular void is controlled in volume and pressure. The choice of the pressure diagram noted P_{grout} (Figure 2) is justified by the position of grout ports (Figures 8b, 9 and 10). The latter are distributed along the perimeter of back shield tail for Lyon and Shanghai cases and located on upper part for Toulouse case. The maximum value of injection pressure is set on maximum vertical displacement recorded on construction site as close to vertical axis of tunnel. It shows in particular that pressure really transmitted to the ground remains lower than the average pressure measured at the exit of injection pipes: this difference is due to pressure loss by friction following the flow of grout as well as to its impregnation of surrounding ground

(Demagh *et al.*, 2008). Uncertainty on the rheology of grout leads to consider two principal stages (liquid and solid stages) intercalated by a transitional one:

- The liquid stage corresponds to incompressible behaviour of the grout in order to fill the annular void and to transmit injection pressure to surrounding ground. This stage is simulated by application of P_{grout} and reactivation of volumetric elements. A pressure gradient is considered in order to take into account not only grout's own weight but also special provisions of injection. During this stage, grout is considered elastic-incompressible (Dias *et al.*, 2000) and is characterized by a high bulk modulus K associated with a low shear modulus G , $10^2 \leq K/G \leq 10^3$ (Bezuijen *et al.*, 2005 and 2006). This stage lasts as long as grout keeps its whole workability, approximately four hours according to (Talmon *et al.*, 2005), which corresponds to average pose of four liner rings.
- The transitional stage corresponds to consolidation of grout. During this stage, the rheology of grout evolves more or less quickly, according to type of grout used (active or inert). More consistent, the grout acquires a shear strength associated with a given compressibility. This stage is simulated by annulment of injection pressure and a progressive reduction in Poisson's ratio (Dierkens, 2005).
- The solid stage corresponds to final situation where grout is at least as rigid as surrounding ground and transmits efforts of ground solid mass to liner (Kasper and Meschke, 2004). This stage is characterized by a ratio $K/G \cong 1$ (Dierkens, 2005).

This procedure is repeated throughout the shield progression, until a stationary section is reached after a few tens of excavation steps which correspond to about 40 m after the passage of front face (Figures 8 and 9). The simulations are carried out with driven shield control parameters recorded during the passage under the measurement sections: drained conditions for Lyon case (effective stresses taking into account buoyant unit weight corresponding to long-term behaviour) and undrained conditions for Toulouse and Shanghai cases (total stresses taking into account water level, which corresponds to short-term behaviour). The simulation results are confronted with in-situ data collected on construction tunnel sites. These data include ground movements on surface and inside the ground solid mass, as well as driven shield control parameters.

4.0 Results

Figure 5 shows Lyon and Shanghai cases (soft normally consolidated soils), the final transverse settlement trough resulting from the simulations seems in agreement with recorded measurements (well represented by the Gaussian distribution), which is also well approached by Peck equation (1969) expressed by Eq. 1:

$$S(x) = S_{\max} \exp(-x^2/2i^2) \quad (1)$$

On the other hand, in Shanghai case (see Figure 5b), the simulated final transverse settlement trough is higher than the observed one; this difference in trough width can be partly explained by:

- i) Proximity of measurement section with respect to entry shaft where surface ground was treated behind (Yan *et al.*, 2008).
- ii) Important uncertainties in distribution of the grouting pressure field inside annular void with a so large diameter TBM (15.4 m).
- iii) Elastic linear/Mohr-Coulomb model, not well adapted for this type of soft soils.

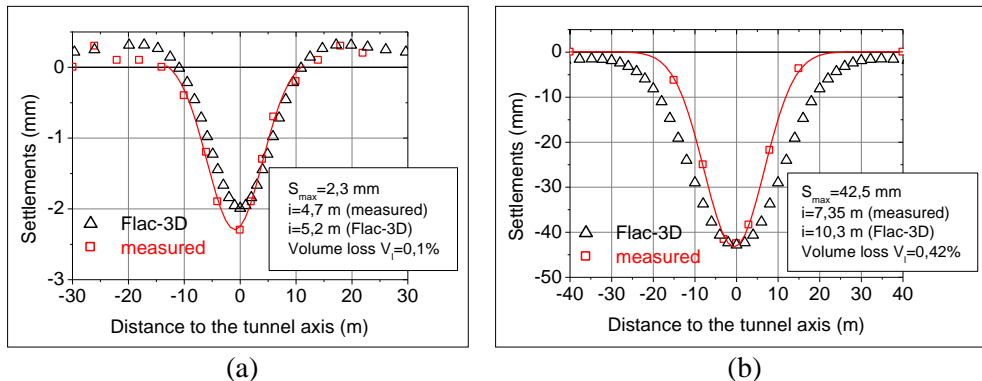


Figure 5: Transverse settlement trough (a) Lyon case (b) Shanghai case

Figure 6 representing Toulouse's case, highly over consolidated excavated soils (K_0 close to 1.7) resulted in heave trough at ground surface with a maximum of approximately 1mm (Figure 6a). This trough is well simulated both qualitatively (evolution during progression of TBM) and quantitatively. Furthermore, final reversed half-width trough is equal to 8 m, and settlement zones seem in agreement with in-situ recorded measurements (Figure 6b).

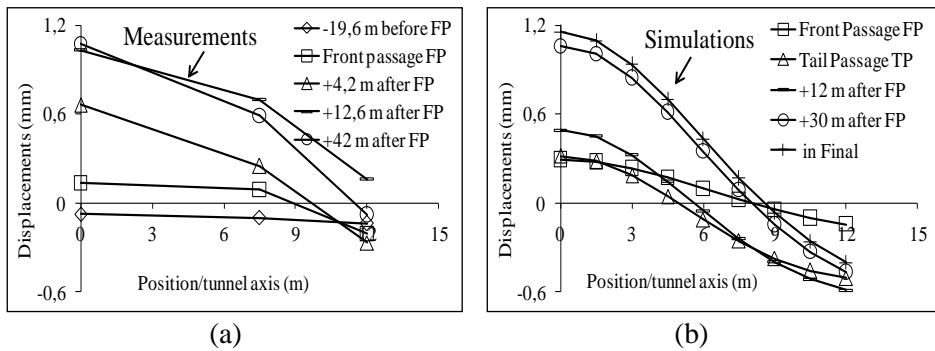


Figure 6: Transverse settlement trough, Toulouse case
 (a) Measurements, (b) Simulations Flac-3D

Figure 7a shows the induced horizontal movements, measured by means of a deep inclinometer on a vertical profile close to tunnel (at one diameter of springline tunnel axis), which are well reproduced too, according to position of shield head and final state; increase of convergence during progression of head shield's is well simulated by the proposed 3D procedure (Figure 7b).

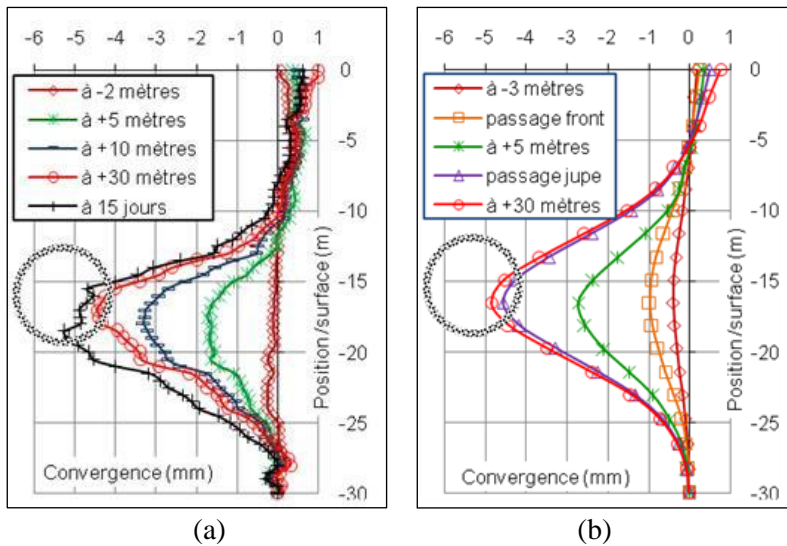


Figure 7: Horizontal convergences, Toulouse case
 (a) Measurements, (b) Simulations Flac-3D

This atypical behavior: 5mm horizontal convergence associated with 1mm of ground surface's heave is essentially due to the over consolidated character of soil crossed and the related K_0 value which is close to 1.7. Nevertheless, variation of a Young modulus law is more appropriate than that proposed in section 2 (Vanoudheusden *et al.*, 2006) which could still refine results of convergence displacements between depths 5 m and 10 m.

Figures 8, 9 and 10 illustrate the 3D ability procedure to describe TBM progression effect through the longitudinal settlement trough. They show relevance of choices for simulation, in particular the injection pressure maximum value, set on vertical displacement of depth point on the central extensometer recorded on construction site. Results are less convincing when values are set on horizontal displacement recorded on the nearest inclinometer (Demagh *et al.*, 2009). In addition, choice of injection pressure distribution is justified by grout ports position at the back of the shield tail. The soil/TBM interaction is thus studied through Figures 8, 9 and 10.

4.1 Lyon Case

The influence of TBM is felt upstream at one diameter before measurements section, a small settlement is then noticed (Figure 8a). Front passage results in an equivalent settlement in Crown Point near tunnel axis and on surface. At front passage, rigid shield prevents any movement of ground convergence; the excavation is thus performed at constant volume. The passage of the tail shield results in an additional vertical displacement of the Crown Point equals to 2mm ($\Delta V_{key}=3mm$), associated with a low additional surface settlement. This shows good control of confining pressure by shield slurry bubble air pressure. Generally, according to (Benmebarek *et al.*, 2000), vertical displacements caused by the front approach and passage of the tail shield represent main cause of vertical movements on surface and which can represent up to 80% of total settlement. These settlements are very low compared to formed gaps behind; this can be explained either by migration of part of grout injected under pressure forward by decreasing ground decompression or by lack of time allowing the soil to close completely the annular void.

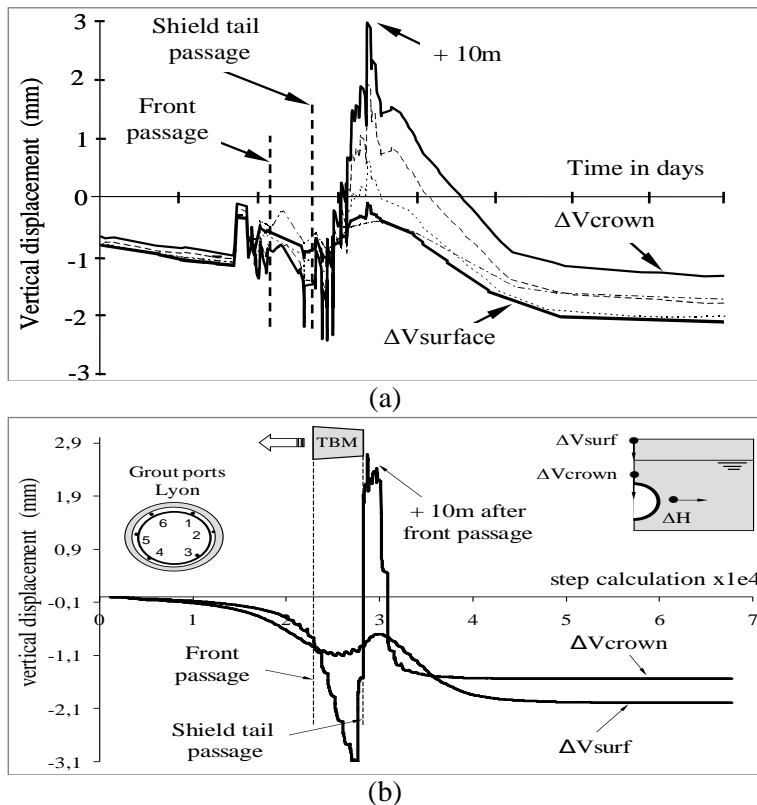


Figure 8: Longitudinal settlement trough, Lyon case
 (a) Measurements, (b) Simulations Flac-3D

Figure 8 shows that injection heaves the crown tunnel point by approximately 3mm above its original position, at 10 m behind the front passage. Maximum effect of injection is felt both in-depth and on surface. It should be noted that vertical movements in-depth and on surface take place simultaneously.

Finally, a stage of deferred settlements which starts after maximum effect of injection is noted. Settlements continue to evolve tending towards an asymptote due to vertical displacements stabilisation.

Figure 8b, vertical displacements are qualitatively well simulated, particularly in final state where surface settlement recorded is more important than maximum vertical displacement measured close to tunnel. Furthermore, after maximum injection, sudden points of settlement ΔV_{crown} associated with a more attenuated points of settlement $\Delta V_{surface}$ can be attributed to simulation procedure itself; during grout consolidation stage, which also corresponds to annulment of injection pressure on excavation perimeter

(Figure 2), a less brutal reduction of injection pressure P_{grout} would involve, in our opinion, a more spread ΔVc_{rown} profile.

The retroactive aspect of injection, between passage of front face and the exhaust of the shield tail, which is though partially known (the shield is not instrumented to record grout pressure upstream of the shield tail), is however relatively well simulated. Indeed, Figure 8b shows that effect of retroactive injection is felt after by a clear movement of heaving of tunnel crown. The maximum displacement is recorded during injection stage at the same time on tunnel crown and surface.

4.2 Toulouse Case

The ground is not disturbed when shield head approaches measurements section, at least until a distance equivalent to one diameter. The front passage results in a small heaving movement on surface associated with a slight horizontal convergence (ΔH in millimetre). The passage of shield tail is characterized by an important horizontal convergence (95% of total convergence) and a low heaving movement on surface is caused by conicity volume loss; this highlights K_0 effect on vertical displacements. Indeed, a parametric study showed that from a given value of $K_0 \geq 1.3$, it is not any more injection which controls movements of surface heaving but K_0 effect would be more dominating (Demagh *et al.*, 2008).

During this stage, the volume loss appears to be stabilized and contrary to what was expected, even with maximum injection, the effect on displacements (in particular horizontal convergence on springline level) is not felt or recorded by measurements. This is confirmed further by displacements profile of Figure 8 where a continuous convergence is observed. This confirms once again state of strong overconsolidation of the “Toulouse’s molasse”, which was not noted in Lyon and Shanghai cases. Otherwise, part of heaving observed on Figure 6, with a stronger slope (Figure 9) can be induced, at least partly, to injection and not only to convergence by K_0 effect.

It is noted for this purpose, that injection pressure adopted in calculations and set on vertical displacement remains lower than half of average pressure measured on four grout ports. It is generally recommended to inject with a pressure threshold slightly higher than initial vertical stress with tunnel crown. The difference in pressure can be explained by a load loss by friction following mortar flow like to its impregnation of surrounding ground.

The grout consolidation is characterized by a small return of point ΔH to its position at the time of shield tail passage, which shows that the proposed procedure to simulate the grout consolidation appears to be relevant. It is further observed that the shifted effect of injection is felt to 30 m compared to monitored section where maximum heaving is

recorded. At the end of last stage (stabilization of displacements), a ratio $\Delta H/\Delta V$ close to 4 is recorded, identical to that recorded on monitored section (Vanoudheusden *et al.*, 2006).

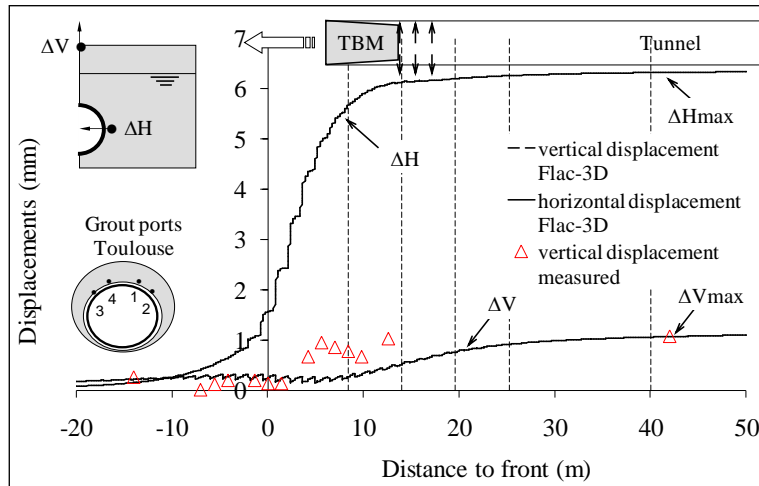


Figure 9: Longitudinal settlement trough, Toulouse case

4.3 Shanghai Case

When shield approaches front passage, a vertical displacement of 10mm occurred and this is equivalent to 20% of total settlement recorded on surface. During this stage, longitudinal settlement trough (Figure 10) is well simulated by calculation, as well as its amplitude that shape. The passage of shield tail results in a volume loss equivalent to an additional surface settlement equals to 35mm. During this stage, simulations are also in good agreement with recorded measurements.

Nevertheless, heaving related to injection of annular void appears more quickly in simulations. The actual grouting pressure distribution is probably different from what has been considered. This can be attributed to a slower heave development after passage of tail (in addition to vicinity of entry shaft and treated zone of soil). This problem is observed differently in Lyon and Toulouse cases where the tunnel boring machines with relatively smaller diameters were used.

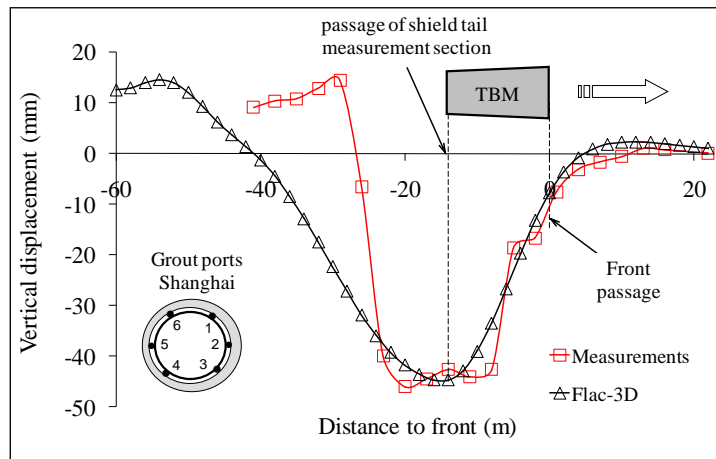


Figure 10: Longitudinal settlement trough, Shanghai case

5.0 Conclusions

A 3D simulation procedure to account for all different operations achieved by a tunnel boring machine (TBM) is proposed in this paper. The procedure has been applied to reproduce by back-analysis movements recorded on three different case studies. The comparison of simulations results with in-situ measurements have shown that the proposed 3D simulation procedure is relevant, in particular in adopted representation of different operations realized by the TBM.

Qualitatively, a good agreement, between displacements evaluated numerically and those recorded in site, was discovered for calculations conducted both in drained or undrained conditions. The obtained ground surface longitudinal and transverse troughs as well as transverse horizontal displacement on vertical profiles agree also well with measurements (final values and evolution during TBM progression). Particularly, singular behaviour of two monitored sections was successfully reproduced. The amplitude of surface settlement is greater than that recorded on deep crown point of tunnel for Lyon P2-S section; this vertical displacement is associated with a movement of divergence on tunnel springline level, on the other hand, in “Castéra” section, similar performances are obtained, the heave trough at ground surface associated with increase and continuous movement of convergence are underlined; this atypical behaviour is partially due to over consolidated character of soil.

These results illustrate the ability of 3D procedure to describe the effects of TBM progression for all movements in 3D space. Nevertheless, if migration of mortar appears to be well simulated by a correction of the conicity, uncertainties related to injection of mortar in different steps still remain difficult to simulate.

In addition to the effect of K_0 , a parametric study will allow to assess the impact of shield control parameters, namely the confining pressure, the injection pressure as well as the position of grout ports and possibly the conicity of the shield to predict tunnelling-induced movements.

References

- Benmebarek, S. and Kastner, R. (2000). *Modélisation numérique des mouvements de terrain meuble induits par un tunnelier*. Revue Canadienne de Géotechnique, 37: 1309-1324.
- Bezuijen, A., Talmon, A.M., Kaalberg, F.J., Plugge, R. (2005). *Field measurements of grout pressure during tunnelling of Sophia Rail Tunnel*. Tunneling. GeoDelft, 83-93.
- Bezuijen, A. et Talmon, A.M. (2006). *Proceedings of the Geotechnical Aspects of Underground Construction in soft Ground, Bakker and al(eds) Taylor & Francis Group, London, 187-193.*
- Broere, W. & Brinkgreve, R.B.J. (2002). *Phased simulation of a tunnel boring process in soft soil*. Numerical Methods in Geotechnical Engineering, Mestat (ed.), Presses de l'ENPC/LCPC, Paris, 529-536.
- Demagh, R., Emeriault F. and Kastner R. (2008). *3D modelling of tunnel excavation by TBM in overconsolidated soils*. JNGG'08 Nantes, 18-20 juin 2008, 305-312 (in French).
- Demagh R., Emeriault E. & Kastner R. (2009). *Shield tunnelling -Validation of a complete 3D numerical simulation on 3 different case studies*. Euro:Tun 2009. Proceedings of the 2nd International Conference on Computational Methods in Tunnelling. Ruhr University Bochum, September 2009, 77-82.
- Demagh R., Emeriault F. & Kastner R. (2009). *Modélisation 3D du creusement de tunnel par tunnelier à front pressurisé – Validation sur 3 cas d'études*. Proceedings of the 17^{ème} Conférence de Mécanique des Sols et de Géotechnique (17^{ème} ICSMGE), 5-9 Octobre 2009, Alexandrie, Egypte, 77-82 (in French).
- Dias, D., Kastner, R. and Maghazi M. (2000). *3D simulation of slurry shield tunnelling*. Proceedings of International Symposium on Geotechnical aspects of underground construction in soft ground, Kusakabe, Balkema, Rotterdam, 351-356.
- Dierkens, M. (2005). *Mesures rhéologiques et modélisation de matériaux en cours de prise*. PhD thesis, INSA-Lyon (in French).
- Kasper, T. and Meschke, G. (2004). *A 3D finite element simulation model for TBM tunnelling in soft ground*. International Journal for Numerical and Analytical Methods in Geomechanics, 28: 1441-1460.
- Kasper, T. and Meschke, G. (2006). *On the influence of face pressure, grouting pressure and TBM design in soft ground tunnelling*. Tunneling and Underground Space Technology, 21: 160-171.
- Mroueh, H. and Shahrour, I. (1999). *Modélisation 3D du creusement de tunnels en site urbain*. Revue Française de Génie Civil, 3 : 7-23 (in French).
- Mroueh H. and Shahrour I. (2008). *A simplified 3D model for tunnel construction using tunnel boring machines*. Tunneling and Underground Space Technology, 23: 38–45.
- Peck RB. 1969., *Deep excavation and tunnelling in soft ground*. In: Proceedings of the 7th International Conference on Soil Mechanics and Foundations Engineering. Mexico City, State-of-Art, 225–290.

- Talmon, A.M., Aanen, L., Bezuigen, A. and van der Zon, W.H. (2005). *Grout pressure around a tunnel lining. Tunnelling. A Decade of Progress. GeoDelft*, 77-82.
- Vanoudheusden, E. *et al.* (2006). *Analysis of movements induced by tunnelling with an earth-pressure balance machine and correlation with excavating parameters*. Proceedings of the Geotechnical Aspects of Underground Construction in Soft Ground, Bakker and al(eds) Taylor & Francis Group, London, 81-86.
- Yan J., Emeriault F., Kastner R. (2008). *Validation d'une procédure de modélisation numérique des mouvements induits par un tunnelier de très grand diamètre dans les argiles molles*. Proceedings of the 26th Rencontres Universitaires de Génie Civil. Nancy, 4 - 6 juin 2008, 8 pages (in French).